

# Experimental study on the flexural behaviour of fibre reinforced concretes strengthened with steel and macro-synthetic fibres

N. Buratti, C. Mazzotti & M. Savoia

*DISTART – Structural engineering, University of Bologna, Bologna, Italy*

**ABSTRACT:** Fibres are widely used to improve the flexural toughness and ductility of concrete, and they may even eliminate the need for conventional reinforcement. Steel fibres are more commonly used in structural applications while synthetic fibres are more often used to reduce crack opening due to shrinkage. Macro-synthetic fibres have been developed with the aim of creating an alternative to steel fibres in structural applications but their use is still limited. The present paper describes the results of an experimental investigation on the performances of concrete specimens reinforced with either steel or macro-synthetic fibres under three point bending. Test results were used to calculate the parameters of stress-crack opening relations via inverse analysis.

## 1 INTRODUCTION

Fibre Reinforced Concrete (FRC), obtained by adding steel or synthetic fibres to plain concrete, is becoming widely used in civil engineering because of its favourable properties (Ahmad et al. 2004). In particular, the introduction of fibres gives to concrete a significant tensile residual strength in the cracked phase and reduces the crack propagation. Fibres are also used to improve the flexural toughness and ductility of concrete. FRC may increase the speed of construction and may even eliminate the need for conventional reinforcement.

The characteristics of FRC depend on the properties of the concrete matrix but mostly on the type, the amount and the geometry of the fibres; these parameters, in fact, control the bond between fibres and concrete.

Nowadays different types of fibres are available to engineers. Steel-Fibre Reinforced Concretes (SFRC) are widely used in a range of structural applications such as: structural facade panels, industrial floors, precast structural elements, tunnel linings, etc., and in general in all those applications in which concrete cracking control is important. Synthetic fibres are usually manufactured in smaller dimensions with respect to steel fibres and most typically used in industrial floors to reduce cracking induced by shrinkage. Recently, Macro-Synthetic Fibre Reinforced Concretes (MSFRC) have been developed with the aim of substituting steel fibres in structural applications but the level of knowledge on their mechanical behaviour is still limited.

This paper describes the results of an extensive experimental campaign performed at Laboratory of Structural Engineering of the University of Bologna. In this campaign several concrete beams were casted using a concrete reinforced with different types and

amounts of steel and macro-synthetic fibres and were tested in a three-point bending scheme.

All the beams were casted using the same concrete mix design. The mix composition was defined in a preliminary experimental campaign, in order to have the desired tensile strength. Data obtained during the tests were used to calibrate the parameters of a stress crack-opening relation by means of an inverse analysis procedure.

## 2 DESCRIPTION OF THE EXPERIMENTAL CAMPAIGN

The following sections describe the most important features of the experimental campaign. All the tests described in this paper were performed following the guidelines given by EN 14651:2005 and EN 14845:2006.

### 2.1 Reference concrete

The mechanical properties of the concrete used in the present study were in agreement with the prescriptions of EN 14845:2006, which specifies four types of reference concrete with given flexural tensile strength, maximum size of the aggregate and maximum cement content. In general, the reference concrete should be selected according to the type of product or system in which the fibre is to be applied, however the standard requires fibre manufacturers to declare the performances of their product in one of the aforementioned four mixes which therefore becomes mandatory and for this reason it was used in the present work. This mix must have flexural tensile strength of  $4.3 \pm 0.3$  MPa, in a three-point bending test.

In order to obtain a mix with the required flexural

Table 1. Mix design of the reference concrete.

Component	Unit	Amount
Cement	kg/m <sup>3</sup>	351.1
Sand (0-2 mm)	kg/m <sup>3</sup>	113.5
Sand (0-5 mm)	kg/m <sup>3</sup>	801.3
Gravel (8-15 mm)	kg/m <sup>3</sup>	674.3
Gravel (15-22 mm)	kg/m <sup>3</sup>	320.4
Water	l/m <sup>3</sup>	174.4
Superplasticizer	l/m <sup>3</sup>	2.68

tensile strength some preliminary tests were performed, in which specimens casted using twelve different mix design were tested in a three-point bending scheme. These mixes were characterized by three different values of water/cement ratio and by four different types of aggregates.

This phase of the study led to the definition of the reference concrete mix with the desired flexural tensile strength. Table 1 gives the mix design and Figure 1 gives the aggregate grading. Aggregates, cement, and water/cement ratio were chosen following the guidelines given by EN 14845:2006.

## 2.2 Test method

The test procedure adopted is consistent with the guidelines given by EN 14651:2005 and EN 14845:2006, according to which 150×150×550 (height × width × length) mm<sup>3</sup> prismatic specimens are to be tested in the three-point bending scheme which is shown in Figure 2. The specimens were notched at mid-span (the height of the notch is 25 mm), in order to control the triggering of the crack. The specimens were cured in moulds, under polyethylene sheeting, for 24 h after casting and then demoulded and cured for further 26 days under water at 20 °C. At the end of the curing period, the specimens were prepared for the test and tested 28 days after casting. The tests characterized the tensile behaviour of fibre reinforced concretes in terms of some residual flexural-tensile-strength values. These values are determined from the load-Crack Mouth Opening Displacement (CMOD) the latter being measured by a omega displacement transducer (see Figure 2). The testing machine operates under displacement control with a constant rate of displacement (CMOD or deflection), and has sufficient stiffness to avoid unstable zones in the load-CMOD curve.

During the tests, the rate of increase of the CMOD was controlled: 0.05 mm/min for CMOD ≤ 0.1 mm and 0.2 mm/min for CMOD > 0.1 mm. All the tests were terminated at CMOD = 4 mm.

Figure 3 shows a generic force-CMOD curve obtained from beam tests. The force-CMOD curve is characterized by a number of reference points: the load at the limit of proportionality,  $F_L$ , which is defined

as the maximum load for CMOD ≤ 0.05 mm, and  $F_1$ ,  $F_2$ ,  $F_3$ ,  $F_4$ , which according to EN14651:2005 are defined as the load values at CMOD = 0.5 mm, CMOD = 1.5 mm, CMOD = 2.5 mm and CMOD = 3.5 mm, respectively.

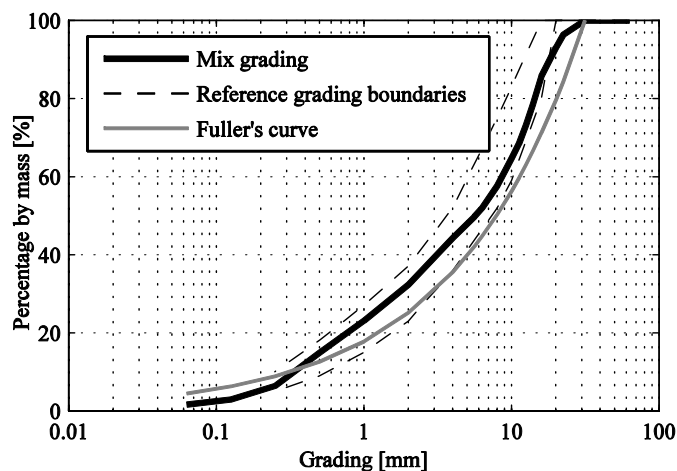


Figure 1. Aggregate grading for the reference concrete. Dashed lines indicate the boundaries of the reference grading given by EN 14845:2006.

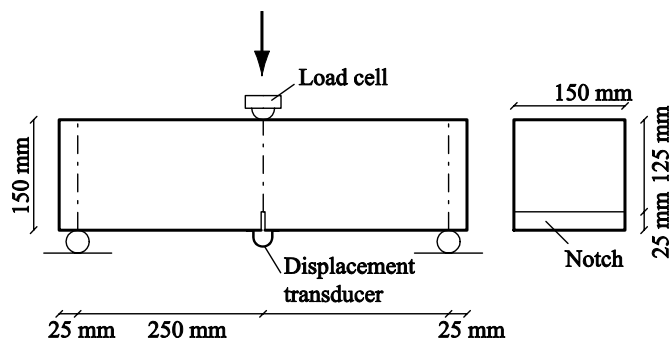


Figure 2. Schematic representation of the experimental set-up.

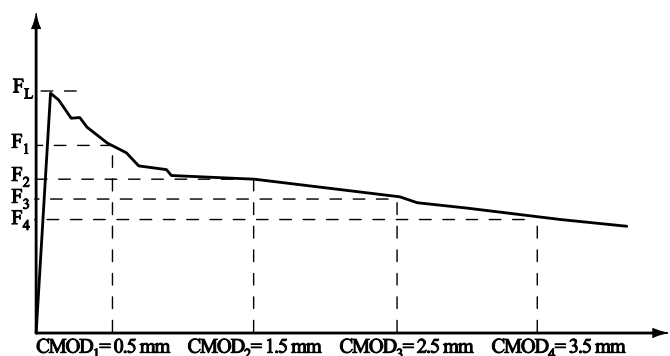


Figure 3. Qualitative representation of a force-CMOD curve and definition of some important points on the curve.

The results of the tests are often expressed also in terms of flexural tensile stress; conventionally obtained by assuming a linear stress distribution over the mid-span cross section, i.e.,  $\sigma = M/W$ , where  $M$  is the mid-span bending moment and  $W$  is the section modulus of the notched section. The flexural tensile strength derived from  $F_L$  is named  $f_{ct,L}^I$ , and the residual flexural tensile strengths derived from  $F_1$ ,  $F_2$ ,  $F_3$ ,  $F_4$  are named,  $f_1$ ,  $f_2$ ,  $f_3$ , and  $f_4$ .

### 2.3 Experimental program

In the present work four different types of fibres were used: three different macro-synthetic fibres and a steel fibre. Figure 4 shows the fibres used and Table 2 gives details on their geometry (length,  $l_f$ , and diameter,  $d_f$ ) and on their mechanical properties (elastic modulus,  $E$ , and tensile strength,  $f_t$ ).

Table 2. Specifications of the fibres used in the present work (data provided by the manufacturers).

Type	Code	$l_f$	$d_f$	$l_f/d_f$	E	$f_t$
		mm	mm			
Steel	SF1B	50	1	50	210	1100
Synthetic	MS1B	54	0.34	158	-	620-758
Synthetic	MS2B	40	0.83	48	11.3	400- 800
Synthetic	MS3B	40	0.44	90	9.5	620

Table 3. Fibre content in the specimens considered.

Mix code	Fibre code	Amount	Volume of fibres
		kg/m <sup>3</sup>	%
MS1B_2	MS1B	2	0.22
MS1B_4_8	MS1B	4.8	0.53
MS2B_5	MS2B	5	0.37
MS2B_10	MS2B	10	0.74
MS3B_2	MS3B	2	0.22
MS3B_4_8	MS3B	4.8	0.52
SF1B_20	SF1B	20	0.26
SF1B_35	SF1B	35	0.45

Two different dosages were used for each type of fibre. Moreover, for each fibre-dosage combination seven beams were casted and tested in a three-point bending scheme. Two cubes (150 x 150 mm) and one cylinder (150 x 300 mm) were casted as well and used to measure the compressive strength and the elastic modulus of the fibre reinforced concretes, respectively.

Gives the dosages, in terms of mass per cubic meter and of volume percentage, considered for each type of fibre. Those dosages were selected in order to be representative, for each type of fibre, of the dosage suggested by the manufacturer and of the maximum dosage recommended to keep a good workability of the fresh concrete, respectively.

In the following, the combinations dosage-type of fibre will be indicated by the codes given in the first column of Table 3. All the specimens were cast using the concrete mix given in Table 1, with the exception of the superplasticizer which in each case was adjusted in order to obtain a slump value of 15-17 cm.

## 3 RESULTS OF THE EXPERIMENTAL CAMPAIGN

This section describes the results obtained during the experimental campaign.

### 3.1 Fresh concrete properties

In order to compare the mechanical properties of the different fibre reinforced concretes considered, the stability of the properties of the concrete matrix among different batches is extremely important. As anticipated in Section 2.1, the reference concrete was defined according to EN 14845:2006. During the casting process, some properties of the fresh concrete were measured: slump (Abrams cone), hydration temperature, and mass.

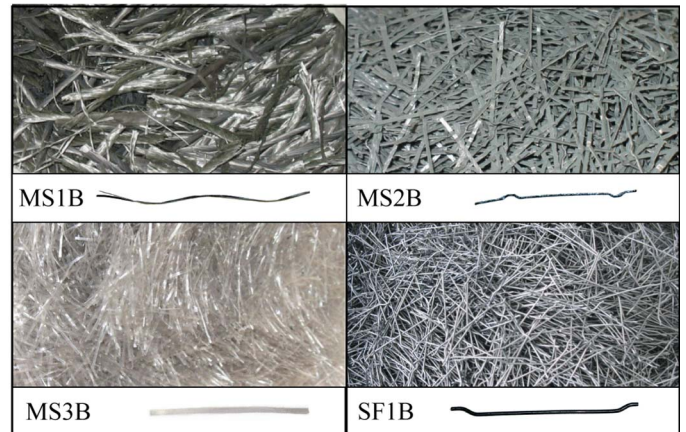


Figure 4. Fibres used in the present study.

Table 4. Properties of the fresh concrete measured during the casting of the different sets of specimens.

Mix code	Additive	Slump	Hydration t.	Density
	l/m <sup>3</sup>	cm	°C	kg/m <sup>3</sup>
MS1B_2	4.73	19	27.5	2434
MS1B_4.8	2.70	17.5	22.6	2454
MS2B_10	3.04	15	23.6	2445
MS2B_5	3.04	15	23.3	2448*
MS3B_2	3.38	15	25.3	2438*
MS3B_4_8	3.38	13	23.7	2426*
SF1B_20	2.70	17	23.2	2462*;
SF1B_35	2.70	16	22.1	2444; 2466*

\* With fibres

Table 5. Elastic modulus and mean compressive strength,  $R_{cm}$ , measured for the specimens of the different sets.

Mix code	Elastic modulus	$R_{cm}$
	MPa	MPa
MS1B_2	37248.9	50.2
MS1B_4_8	30418.2	42.8
MS2B_5	31271.1	40.9
MS2B_10	32171.0	42.1
MS3B_2	-	41.4
MS3B_4_8	-	44.6
SF1B_20	-	41.6
SF1B_35	-	41.7

The so obtained values are listed in Table 4 and show very little variability among the different batches.

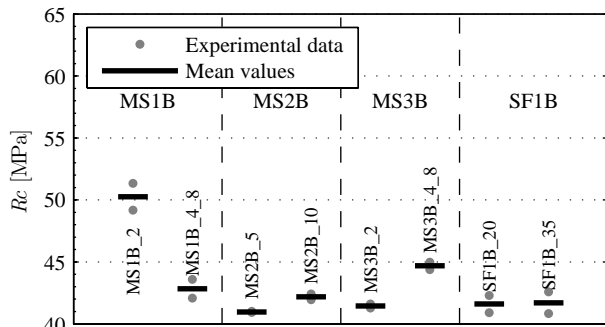


Figure 5. Concrete compressive strength.

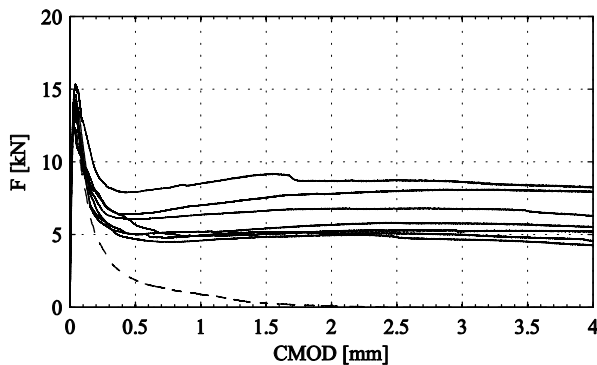


Figure 6. Set SF1B\_20: force CMOD curves. The dashed line indicates the force-CMOD curve for a plain-concrete specimen.

For some of the fibre reinforced concretes, the workability was also measured using the Vebe test, which gave results of about 2 seconds. The properties of the fresh concrete were stable among all the casts.

### 3.2 Mechanical properties of the concrete

For each fibre reinforced concrete mix, two cubes (150 x 150 mm) were casted, and after 28 days of water curing, they were tested to obtain the compressive strength. All the specimens, with the exception of those from the MS1B\_2 set, gave very similar values of compressive strength (see Figure 5), with a mean value of 42.2 MPa and a coefficient of variation of 0.031.

The elastic modulus of the reinforced concrete was measured as well; its values are given in Table 5, together with the compressive strengths.

Accordingly to the results obtained in the compressive tests, the concrete of the MS1B\_2 set had an elastic modulus higher than average.

### 3.3 Results of three point bending tests

As previously stated, load and CMOD values were measured in each test. As an example, Figure 6 shows the curves obtained for the specimens of the set SF1B\_20 (steel fibres) and a force-CMOD curve for a plain-concrete specimen tested during the concrete-mix definition phase (dashed line).

As widely known, the addition of fibres to concrete does not significantly increase the tensile strength, but greatly enhances the concrete toughness. It is worth

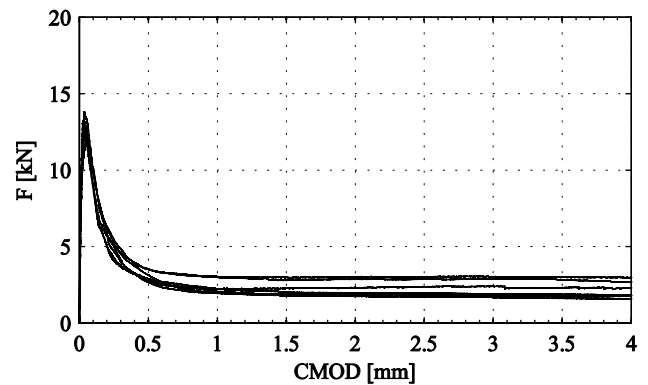


Figure 7. Set MS3B\_2: force-CMOD curves.

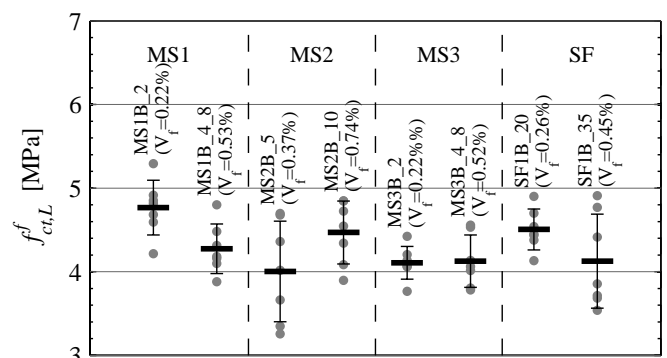


Figure 8. Flexural tensile strengths at the limit of proportionality (MS: Macro-Synthetic fibres; SF: Steel Fibres).

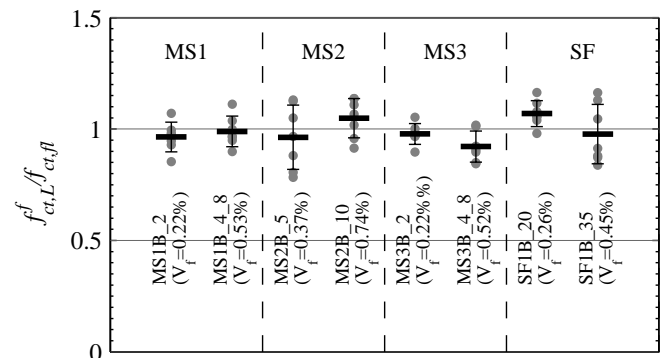


Figure 9. Normalized flexural tensile strengths at limit of proportionality (MS: Macro-Synthetic fibres; SF: Steel Fibres).

noting that the scatter of the force-CMOD curves is usually significant: as it will be discussed in the following, this circumstance, unavoidable using the test method prescribed by EN 14651:2005, is mainly due to the variability of the number of fibres crossing the crack. The dispersion of results in three-point bending beam test strongly depends on the type and amount of fibres; as an example, Figure 7, shows the force-CMOD curves for the specimens of the set MS3B\_2 (macro-synthetic fibres). Comparing Figure 6 with Figure 7 it can be easily seen that the scatter of the experimental results in the post-peak region is much smaller for the specimens with the MS fibres than for the SF specimens.

In the following, the results of the tests will be given in more concise form in order to allow a better comparison among the performances of the different fibre reinforced concretes. Figure 8 shows the flexural tensile strength at the limit of proportionality,  $f_{ct,L}^f$ , for the different specimens. Gray dots indicate actual data points, thick black lines the average values, and thin black lines the  $\pm 1\sigma$  intervals. It is worth noting that the measured values of  $f_{ct,L}^f$  are quite close and their average values fall into the interval  $4.3 \pm 0.3$  MPa as required by EN 14845-1:2006. As previously observed in terms of compressive strength and elastic modulus, the specimens of the set MS1B\_2 had slightly better mechanical properties also in terms of  $f_{ct,L}^f$ .

In order to allow a better comparison between the results, the effects of variability of mechanical properties of the concrete have been reduced by normalizing the  $f_{ct,L}^f$  values with respect to the flexural tensile strength value,  $f_{ct,L}^f$ , predicted by the equation proposed by Model Code 90, which is a function of the compressive strength (see Table 5 for compressive strength values obtained in the present work).

Figure 9 shows the normalized flexural tensile strength values. It is not possible to find any trend between this mechanical parameter and the fibre amount. This confirms that the fibres do not increase the concrete tensile strength; on the contrary an excessive amount of fibres may decrease this strength, as a consequence of a reduction of workability.

The residual flexural tensile strength values ( $f_1, f_2, f_3, f_4$ ) have been compared as well. They have been normalized with respect to the flexural tensile strength,  $f_{ct,L}^f$  and are reported in Figure 10. It can be observed that the residual strengths of the sets containing steel fibres (SF) are usually higher than those of the beams containing macro-synthetic fibres (MS1B, MS2B, and MS3B). The relative strengths of the different sets of beams do not significantly change from  $f_1$  to  $f_4$ , i.e. for increasing values of CMOD. Obviously, the residual strength is higher when a higher amount of fibres is added to the concrete mix.

The scatter of the strength values is higher for steel fibre reinforced concretes, as previously anticipated. This dispersion is due to size of the specimen cross-section, which is small with respect to the amount of fibres (see Section 3.4).

Figure 11 shows a plot of the mean normalized residual strength at various crack openings for each set. It clearly shown that the performances of the steel fibres are usually better than those of synthetic fibres. Nevertheless in design problems characteristic values are commonly used instead of mean values. These characteristic values take into account also the dispersion of the experimental data, therefore if the characteristic residual strengths of the different sets are compared, as done in Figure 12, the benefit given by the steel fibres is reduced.

Finally, for each specimen the toughness index was calculated as well. Since data for the plain concrete specimens were available (collected during the preliminary phase), the toughness index was assumed as the ratio of the area under the force-CMOD curve

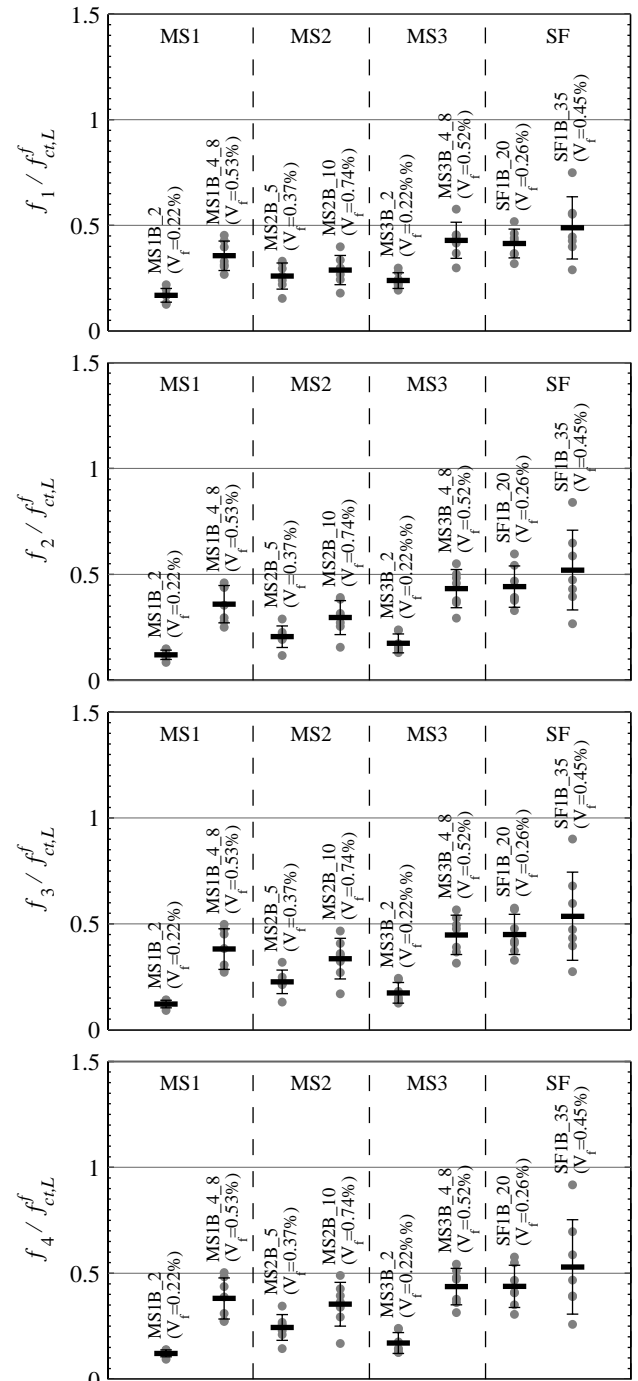


Figure 10. From top to bottom, normalized residual strengths at: CMOD = 0.5 mm; CMOD = 1.5 mm; CMOD = 2.5 mm; CMOD = 3.5 mm.

for the fibre reinforced specimen over the area under the same curve for the plain concrete specimen (Gopalaratnam & Gettu, 1995). Different plain concrete specimens manufactured from the reference mix were tested and therefore the average value of the areas under their force-CMOD curves was used. The values of the toughness index are shown in Figure 13.

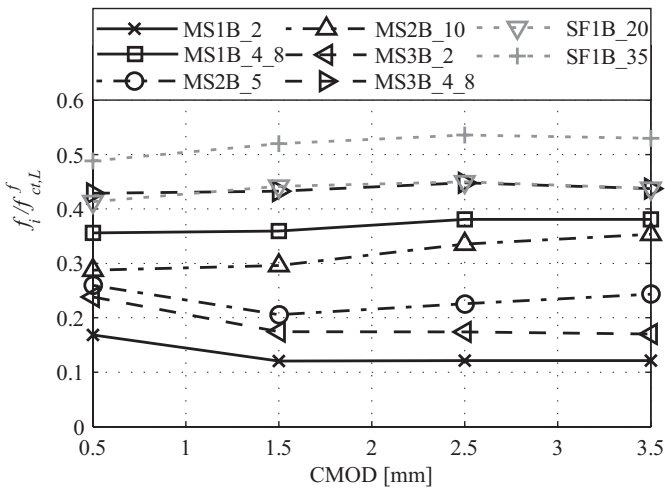


Figure 11. Average strengths at different CMOD values for the sets of specimens with different types and amount of fibres.

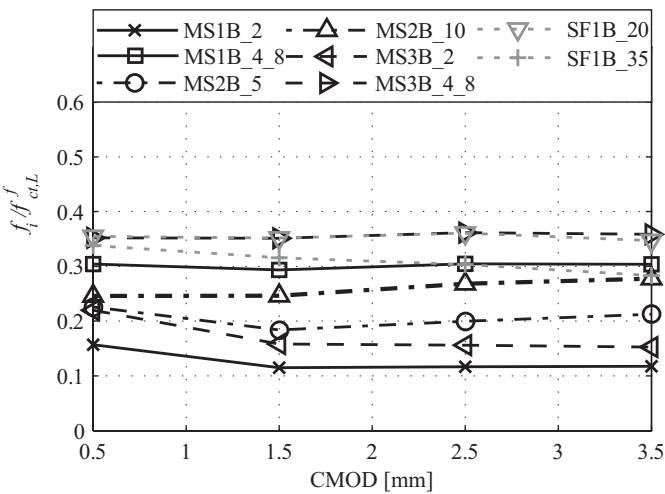


Figure 12. Characteristic strengths at different CMOD values for the sets of specimens with different types and amount of fibres.

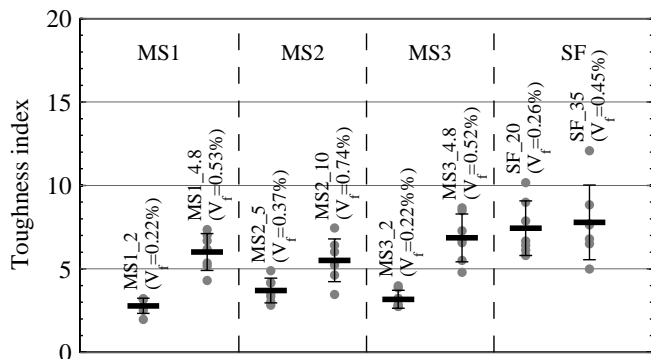


Figure 13. Toughness indexes.

The distribution of the values of the toughness index is very similar with that of the residual strength. It is worth noting that the addition of fibres to concrete can increase its toughness from 5 to 10 times.

### 3.4 Correlation between residual strength and number of fibres

To better understand the reasons of the high scatter of the results obtained for some types of fibres, the number of fibres crossing the crack were determined. When CMOD increased over 4 mm, the transducers were removed from

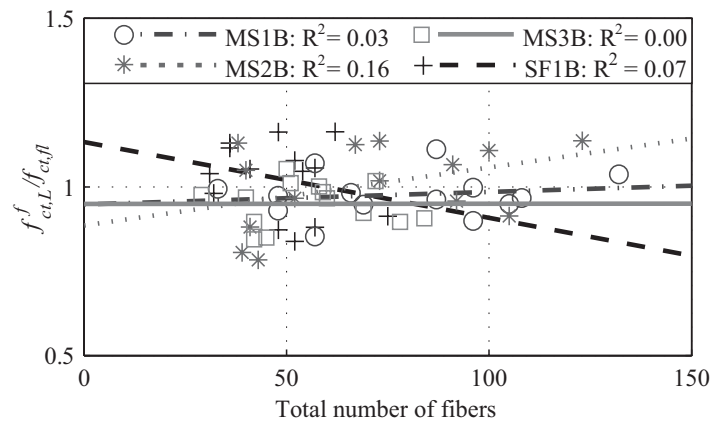


Figure 14. Correlation among normalized strength at the limit of proportionality and the total number of fibres in the crack propagation surface.

the specimen to preserve their integrity and then the test was carried out until the specimen tore apart. The fibres on the two faces of the crack were then counted distinguishing between broken fibres and pulled-out fibres.

The cross-section of the specimen was divided into three horizontal zones with equal height and the number of fibres was counted in each of them. These data were then used to find a correlation between each residual strength value and the number of fibre in each zone of the cross section. For the sake of brevity, here only the correlation with the total number of fibres is considered. Figure 14 gives the normalized  $f_{ct,L}^f$  values versus the total number of fibres. The symbols represent observational data while the lines represent the results of linear regression analysis. This plot confirms that fibres have little influence on flexural tensile strength. In particular the coefficient of determination  $R^2$ , whose values are given in the legends, is very close to 0 for all the sets of specimens.

On the contrary, residual strengths,  $f_1, \dots, f_4$  are strongly correlated with the number of fibres. Figure 15, shows flexural strength values at different CMOD values versus the total number of fibres. The values of  $R^2$  are given in the legend. Obviously, the slope of the lines depends on the strength of the fibres and therefore is higher as far as steel fibres are concerned. This correlation explains the high variability of the results. In fact, Figure 16 shows the total number of fibres for all the specimens considered in the present study and shows that the  $\pm 1\sigma$  intervals are wide for steel fibre reinforce concrete specimens. Furthermore, the intervals for the two dosages considered are strongly overlapped.

On the contrary, as far as macro-synthetic fibres are concerned, the  $\pm 1\sigma$  intervals corresponding to the two dosages considered in the present study are usually non-overlapping.

The distribution of fibres in the mid-span section obviously depends on fibre dosage, fibre geometry and specimen size (Soroushian, 1990): therefore the great dispersion of results can be caused by the fact that the size of the specimen is too small with respect to the dosage of fibres and to their dimension.

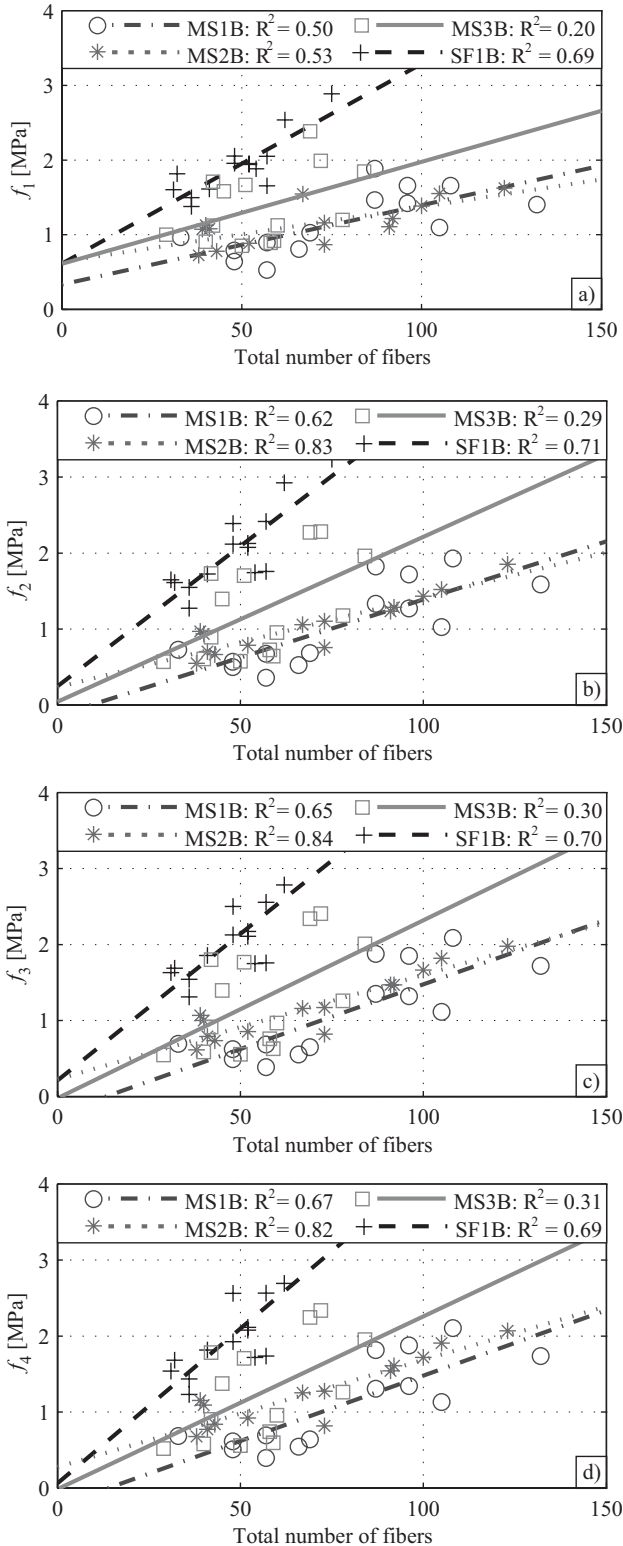


Figure 15. Correlation among residual strengths at different CMOD values and the total number of fibres in the cracked surface.

## 4 STRESS CRACK-OPENING RELATIONS

Data obtained from experimental the tests were used to define, for each type and amount of fibre, the parameters of a stress-crack opening constitutive diagram. Inverse analysis was used to obtain such parameters. In the following the adopted model and the obtained constitutive behaviours will be described.

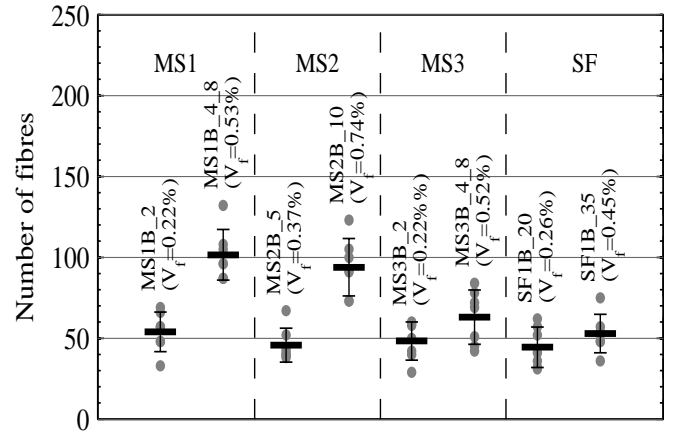


Figure 16. Total number of fibres in the crack propagation section of the specimens.

### 4.1 Model

Many models describing the mechanical behaviour of FRC behaviour with different degrees of accuracy and complexity can be found in the literature. In the present work, a simplified model has been adopted, in order to have a more direct as possible connection between the experimental results obtained from the test specimens and those required for the design of fibre reinforced structural elements. In fact, since the CMOD-stress relationship is not a constitutive relationship, i.e. is not an intrinsic property of the material, the relationships obtained through inverse analysis depend on the model selected.

The cracked hinge model used in the present work has been proposed by Olesen (2001) and describes the bending failure of a FRC beams by the development of a fictitious crack. The basic idea of the cracked hinge is to model the portion of the beam close to the propagating crack as a layer constituted by horizontal strips, attached at the two ends to rigid boundaries which can rotate. The strips are then modelled as independent spring elements with non linear constitutive behaviour. With this approach, the disturbance of the strain field, caused by the presence of the crack, is confined to take place between the rigid boundaries. The two rigid boundaries may translate and rotate, so constituting a non linear spring which can be joined with uncracked beams modelled according to the classical beam theory. The constitutive relation of the spring layer is the same as that of the FRC. Olesen's model uses a bilinear stress-crack opening relation, shown in Figure 17 to describe the spring layer behaviour.

### 4.2 Inverse analysis formulation

The inverse analysis procedure has been used in order to find the values of the parameters defining the stress-crack opening relation -  $f_i$ ,  $\sigma(w_1)$ ,  $w_1$  and  $w_2$  (see Figure 17) - that together with the Olesen's model, allow to best re-produce the test results. The

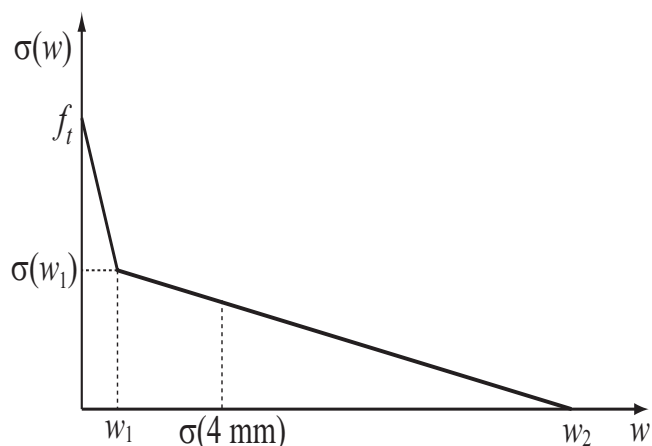


Figure 17. Stress-crack opening relation used in the Olesen's model (Olesen, 2001).

length of the non-linear hinge should be considered a fitting parameter for the calculations because, in general, it depends on the type of structural element. In the present work, according to Olesen (2001) and RILEM TC 162-TDF (2002), it was assumed that the length of the hinge is 0.5 times its height; this latter parameter is set equal to the net section height.

The optimal values of the aforementioned parameters were determined using Matlab's optimization algorithms. The objective function to be minimized by the algorithm was defined as a weighted sum of the squared residuals between experimental and numerical results at some CMOD opening values. In particular the values considered are: the area under the force-CMOD diagram in the interval  $0.05 < \text{CMOD} < 4 \text{ mm}$ , the force at limit of proportionality and the residual strengths at CMOD values of 0.05, 0.1, 0.2, 0.5, 1.5, 2.5, and 3.5 mm.

#### 4.3 Results of the inverse analysis

Table 6 gives, for each set of specimens, the average values and the coefficients of variation of the parameter values obtained from the inverse analysis. Since the tests were stopped at  $\text{CMOD} = 4 \text{ mm}$ , to make clear the limit of validity of the results, the flexural tensile stress at 4 mm,  $\sigma_w(4 \text{ mm})$ , is given instead of  $w_2$ ; this latter parameter was always significantly greater than 4 mm. Inverse analysis was used on all the experimental results, obtaining in general a good accuracy of the results. In particular, the stress-crack opening relations obtained produce force-CMOD diagrams providing good approximations of all the experimental diagrams in terms of all the measures considered in the optimization process. The match of numerical diagrams with experimental ones is worse in the curve portion straight after the peak: the steeper the curve the lower the match. Errors in the predictions of Olesen's model, calculated as relative difference among experimental and numerical values, are very low as far as the force at limit of proportionality

Table 6. Mean values and coefficients of variations of the parameters of the stress-crack opening relations (see Figure 17) obtained by inverse analysis.

Mix code		$w_1$	$f_t$	$\sigma_w(w_1)$	$\sigma_w(4 \text{ mm})$
MS1B_2	Mean	0.07	2.70	0.19	0.17
	COV	0.10	0.11	0.23	0.25
MS1B_4_8	Mean	0.06	2.39	0.50	0.50
	COV	0.13	0.12	0.21	0.21
MS2B_5	Mean	0.07	2.23	0.29	0.29
	COV	0.19	0.20	0.23	0.24
MS2B_10	Mean	0.05	2.64	0.47	0.47
	COV	0.18	0.11	0.27	0.27
MS3B_2	Mean	0.07	2.04	0.23	0.16
	COV	0.16	0.30	0.38	0.75
MS3B_4_8	Mean	0.07	2.28	0.61	0.59
	COV	0.36	0.12	0.22	0.27
SF1B_20	Mean	0.05	2.40	0.60	0.60
	COV	0.16	0.25	0.34	0.34
SF1B_35	Mean	0.05	2.21	0.67	0.66
	COV	0.24	0.16	0.33	0.35

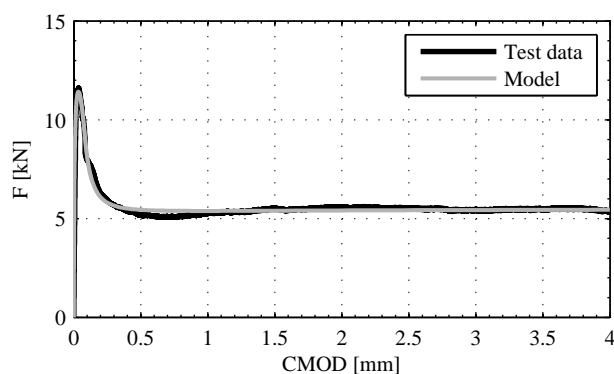


Figure 18. Comparison between an experimental force-CMOD curve and that obtained after the inverse analysis.

(less than 2%) and the area under the diagram (less than 1%) are concerned while they are greater in terms of residual strengths: 15% on average for  $f_1$  and 5% on average for  $f_2$ ,  $f_3$ , and  $f_4$ . As an example, Figure 18 shows a comparison between the numerical and the experimental force – CMOD diagrams for one specimen of the set named SF1B\_35. In this case the model gives very good predictions especially in the latter part of the curve. For very low crack opening values the accuracy of the results is lower. The accuracy might be increased by using more complex force-crack opening relations.

## 5 CONCLUSIONS

The present work investigated the flexural behaviour of notched beams made of concretes fibre-reinforced with different types and amounts of fibres. Steel fibres showed generally better performances than macro-synthetic fibres but with a greater scatter of force-CMOD curves.

The experimental data were used as input for inverse analysis which lead to the optimal bilinear stress-crack opening relations to be used with Olesen's model in order to reproduce the experimental behaviour of the beams.

## ACKNOWLEDGEMENTS

Financial support of the Technical Consortium of steel fibre producers is gratefully acknowledged.

## REFERENCES

Ahmad, A. Di Prisco, M. Meyer, C. Plizzari, G.A. & Shah, S.P. 2004. *Fiber reinforced concrete: from theory to practice*, Bergamo, 24 - 25 September.

- De Oliveira e Sousa, J.L.A. & Gettu, R. 2006. Determining the tensile stress-crack opening curve of concrete by inverse Analysis. *Journal of Engineering Mechanics* 132(2): 141-148.
- EN 14651:2005 2005. *Test method for metallic fibered concrete - Measuring the flexural tensile strength (limit of proportionality (LOP), residual)*.
- EN 14845:2006 2006. *Test methods for fibres in concrete*.
- Gopalratnam, V.S. & Gettu, R. 1995. On the characterization of flexural toughness in fiber reinforced concretes. *Cement and Concrete Composites* 17(3): 239-254.
- Olesen, J.F. 2001. Fictitious crack propagation in fiber-reinforced concrete beams. *Journal of Engineering Mechanics* 127(3): 273-280.
- RILEM TC 162-TDF 2002. Test and design methods for steel fibre reinforced concrete. Design of steel fibre reinforced concrete using the  $\sigma$ -w method: principles and applications. *Materials and Structures* 35(5): 262-278.
- Soroushian, P. & Lee, C.-D. 1990. Distribution and orientation of fibres in steel fiber reinforced concrete. *ACI Materials Journal* 87(5): 433-439.